

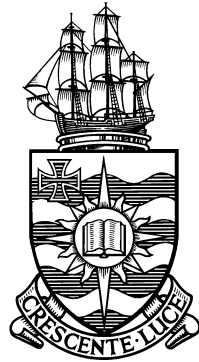
Computational and Experimental Modelling of the Crushing of Prepared Sugar Cane

Thesis submitted by

Arasu Kannapiran

B.E., University of Madras, India

M.Tech., Indian Institute of Technology, Madras, India



in September 2003

for the degree of Doctor of Philosophy

in the School of Engineering (Mechanical Engineering)

James Cook University of North Queensland

STATEMENT OF ACCESS

I, the undersigned, the author of this thesis, understand that James Cook University of North Queensland will make it available for use within the University Library and, by microfilm or other means, allow access to users in other approved libraries. All users consulting this thesis will have to sign the following statement:

In consulting this thesis I agree not to copy or closely paraphrase it in whole or in part without the written consent of the author; and to make proper public written acknowledgement for any assistance that I have obtained from it.

Beyond this, I do not wish to place any restriction on access to this thesis.

(Arasu Kannapiran)

Date _____

ABSTRACT

This thesis presents the investigation and application of porous media mechanics and elasto-plastic constitutive theory for the crushing of prepared sugar cane using finite element simulation. This research specifically investigates the experiments carried out on C. R. Murry Advanced Experimental Milling Facility using cane that has also passed through a series of basic tests to characterise its properties for the computational models. For isotropic plastic material behaviour, constitutive models that represent yielding under hydrostatic pressures are applied. The constitutive behaviour of the solid skeleton, and the plastic strain hardening response are derived from a series of slow speed confined uniaxial compression experiments. The liquid flow within fibrous solid matrix of prepared cane is modelled by applying Darcy's law, and the coefficient of permeability therefore was determined experimentally.

The finite element technique applied to the crushing process, couple the elasto-plastic constitutive theory for the solid fibre and the Darcy's liquid flow theory for the liquid juice in conjunction with the frictional relation between the roller and blanket material. The material law has been coded initially into a two-dimensional plane strain computer model.

Series of experiments on two-roll mill was conducted. The two-dimensional plane strain model predicted the roll load in agreement with experimental values, however failed to capture the tangential component of compression and the torque values were 50% lower than the experimental values. However, numerical prediction of a flat roll surface matched well in roll load and torque with experimental values as the stress levels associated with grooves are absent. The rolls were then modelled with grooves in three-dimension. The three-dimensional model captured high and low compression regions in groove tip and base respectively. The roll loads as well as roll torques matched well with experimental values.

STATEMENT ON SOURCES

I declare that this thesis is my own work and has not been submitted in any form for another degree or diploma at any university or other institution of tertiary education. Information derived from the published or unpublished work of others has been acknowledged in the text and a list of references is given.

(Arasu Kannapiran)

Date _____

ACKNOWLEDGEMENTS

The author wishes to thank gratefully the following people for their valuable contributions to the present study:

Associate Professor Jeffrey Loughran, for his encouragement and invaluable guidance throughout the research project as a supervisor.

Sugar Research Development Council (SRDC) of Australia, for financial support and encouragement throughout the project.

Dr. Clayton Adam, QUT for his valuable notes and discussions on the important aspects of this research.

Dr. Kai Duan, UWA for the useful discussions during initial stage of computation.

Mr. Geoff Kent, Dr. Christopher Downing and Mr. Neil McKenzie of Sugar Research Institute (SRI), Mackay for the useful discussions during initial experimental stage.

Mr. David Kauppila and Mr. Paul Britton of Mechanical engineering, and Mr. Gordon McNealy, Mr. Warren O'Donnell and Mr. Stuart Petersen of School of Engineering for all their technical assistance during grooved and flat roll mill experiments.

Contents

Chapter

1	Introduction	1
1.1	Sugar production processes	1
1.2	Australian sugar industry	2
1.3	Mill rollers	3
1.4	Specific objectives of current investigation	5
2	Literature review and the theory of sugar cane crushing	7
2.1	Nature of prepared sugar cane	7
2.2	Early research (1900-1950)	9
2.3	Fundamental properties of prepared sugar cane (1950-1990)	10
2.3.1	Treatment number	11
2.3.2	Theoretical juice extraction	12
2.3.3	Reabsorption in sugar mills	12
2.4	Fundamental theory of crushing mechanics	15
2.4.1	Early mill experiments	15
2.4.2	Two-roll mill geometry	16
2.4.3	Determination of roll load and roll torque	18
2.5	Prepared cane as a deformable porous media	23
2.5.1	Darcy's law	25
2.5.2	Effective stress	28
2.6	Continuum approach	30

2.6.1	Theory of stresses	31
2.6.2	Stress invariants	34
2.6.3	Concept of strain and of state of strain	35
2.6.4	Plane stress and plane strain	37
2.7	Theory of elasticity	37
2.7.1	Generalized Hooke's law	37
2.8	Plasticity	39
2.9	Approach to modelling	40
2.9.1	Yield criteria	40
2.9.2	Maximum shear stress (Tresca) criterion	41
2.9.3	Shear strain energy (von Mises) criterion	42
2.9.4	Mohr-Coulomb yield surface	46
2.9.5	The Drucker-Prager yield surface	48
2.9.6	Cap models	50
2.10	Critical state theory	51
2.10.1	Cam-clay critical state model	55
2.10.2	Yielding of Cam-clay	57
2.11	Governing equations and finite element solution	61
2.11.1	Overall equilibrium equations	61
2.11.2	Equilibrium equation of liquid	62
2.11.3	Liquid flow continuity equation	62
2.11.4	Stress, pressure, displacement and strain	62
2.11.5	The finite element transient solution	63
2.11.6	Spatial discretization of governing equations	65
2.12	Summary	67

3	Quasi-static uniaxial experiments	68
3.1	Introduction	68
3.2	Scope of quasi-static uniaxial experiments	68
3.3	Testing apparatus and equipment	69
3.3.1	Confined uniaxial compression cell	69
3.3.2	Cane mass and preparation	70
3.3.3	Cane fibre determination	72
3.4	Experimental scheme	73
3.4.1	Uniaxial testing machine	78
3.4.2	Testing procedure	79
3.5	Quasi-static experimental response	81
3.6	Uncertainty in experimental measurement	84
3.6.1	Uncertainty in compression ratio	84
3.6.2	Uncertainty in vertical stress	85
3.7	Compression and volume change	85
3.7.1	Drained conditions in uniaxial compression	85
3.7.2	One-dimensional compression and swelling	87
3.7.3	Interpretation of one-dimensional test results	88
3.7.4	Determination of logarithmic bulk moduli	89
3.8	Summary	91
4	Liquid flow through fibrous matrix	92
4.1	Introduction	92
4.2	Darcy's law and permeability	93
4.3	Permeability based on empirical equations	94
4.4	Permeability response from experiment	95
4.5	Effective permeability	96

4.6	Permeability response from dynamic compression tests	97
4.7	Permeability tests	99
4.7.1	Uncertainty in permeability	101
4.7.2	Permeability results	101
4.8	Discussion of results	104
5	Constitutive formulations for the fibre	106
5.1	Introduction	106
5.2	Experimentally observed material responses	107
5.2.1	Approach to modelling	107
5.3	Simple constitutive equations	109
5.4	Elasticity	110
5.4.1	Linear elasticity	110
5.4.2	Porous elasticity	111
5.4.3	Elastic strains	111
5.4.4	Elastic material parameters	113
5.5	Plasticity	114
5.5.1	Plastic flow	115
5.5.2	Hardening law	116
5.5.3	Calculation of plastic strains for Cam-clay	118
5.5.4	Complete constitutive equation for simple Cam-clay	120
5.5.5	Capped Drucker-Prager plasticity model	121
5.5.6	Determination of plastic material parameters	122
5.5.7	Strain hardening results from quasi-static experiments	129
5.6	Conclusions	133
6	Finite element implementation of coupled model in ABAQUS	135
6.1	Introduction	135

6.2	Coupled porous and elasto-plastic approach	136
6.3	Fundamental methodology of finite element analysis	137
6.4	ABAQUS general purpose finite element programme	138
6.4.1	Components of an ABAQUS model	139
6.5	Mesh and element dependent study	149
6.5.1	Effect of mesh density	149
6.5.2	Effect of element type	149
6.5.3	Mesh refinement results	151
6.6	Adaptive mesh refinement or rezoning	152
6.6.1	Grid or mesh generation	153
6.6.2	Mesh generation procedure in ABAQUS for rezoning	154
6.6.3	External mesh generation	156
6.6.4	Summary	159
7	Two-roll mill experiments and validation	161
7.1	Introduction	161
7.2	Two-roll (Grooved) experimental programme	162
7.2.1	Advanced experimental two-roll milling facility	162
7.2.2	Mill control, instrumentation and measurements	163
7.2.3	Experimental scheme	163
7.3	Pressure distribution due to juice flow	164
7.3.1	Roll load and roll torque estimation	168
7.3.2	One-dimensional frictional theory results	169
7.4	Modelling considerations	171
7.4.1	Initial compression ratio of the blanket	173
7.4.2	Appropriate form of permeability response	174
7.4.3	Boundary conditions	176

7.4.4	Friction factor	177
7.5	Mesh distortion and feeding	178
7.6	Two-roll experimental results and predictions	180
7.6.1	Comparison of results with other experiments	183
7.6.2	Other predicted output parameters	185
7.7	Parameter sensitivity of elasto-plastic property responses	189
7.8	Flat roll mill experiments	192
7.8.1	Flat roll mill experimental plan and input conditions	192
7.8.2	Issues in the numerical modelling of flat-roll milling	195
7.8.3	Numerical modelling results	195
7.9	Conclusions	198
8	Three-dimensional simulation of rolling	200
8.1	Introduction	200
8.2	Three-dimensional surfaces of revolution	200
8.3	Input parameters in three-dimensional simulation	201
8.4	Results from three-dimensional analysis	202
8.4.1	Roll load and roll torque in a 3-D modelling	204
8.5	Conclusions	208
9	Advanced milling simulations	210
9.1	Introduction	210
9.2	Geometry of a three-roll mill	210
9.3	Three-roll mill crushing simulation and results	213
9.3.1	Rezoning during three-roll simulation	216
9.4	Conclusions	217

10 Conclusions	218
10.1 Introduction	218
10.2 Basic property tests and two-roll mill experiments	218
10.2.1 Quasi-static uniaxial tests	219
10.2.2 Permeability responses	219
10.2.3 Two-roll mill experimental results	220
10.3 Flat roll experiments	220
10.4 Rezoning studies	221
10.5 Three-dimensional simulation of grooves	221
10.6 Demonstration of three-roll mill simulation	222
Bibliography	223
Appendix	
A Fortran programme for roll load and roll torque (One-dimension)	227
B Matlab programme to generate mesh for rezoning	230
C ABAQUS programme for three-roll crushing simulation	232
D ABAQUS programme for 3-dimensional simulation	237

Tables

Table

3.1	Dimensions of grooves	70
3.2	Experimental correlation for flat platen	75
3.3	Experimental correlation for 35° grooved platen	78
3.4	The Logarithmic moduli λ and κ	90
4.1	Uncertainty in the measured variables	101
4.2	Experimental correlation of permeability responses	103
5.1	Quasi-static experimental parameters	130
5.2	Elasto-plastic properties of fibrous material	132
6.1	Roll loads for different elements and mesh densities	151
6.2	Mesh refinement results for CPE8RP elements	152
7.1	Work openings for the two roll experiment	164
7.2	Parameters for the two roll experiment	165
7.3	Feeding velocities at different compression ratio	180
7.4	Parameters varied for the numerical experiment	189
7.5	Summary of numerical experiment	191
7.6	Parameters for the two roll (flat) mill experiments	193
7.7	Two-roll (flat) mill operating parameters	194
8.1	Blanket parameters used for 3-D simulation	202
9.1	Parameters used for three-roll simulation	213

Figures

Figure

1.1	Circumferential grooving	4
1.2	Schematic diagram of a six-roll crushing unit	4
2.1	Portion of inter node transverse section	7
2.2	Prepared cane	8
2.3	Juice flow	17
2.4	Pressure distribution	20
2.5	Forces on roll surface	21
2.6	Constituents of sugar cane	24
2.7	Unit volume soil model	25
2.8	Flow through soil	26
2.9	The principle of effective stress	28
2.10	Contact area in soil	30
2.11	Normal tensile load	32
2.12	Multidimensional forces	32
2.13	Triaxial elemental stresses	33
2.14	Planes of stresses	35
2.15	Normal and shear strains	36
2.16	Stress-strain curve typical to metals	39
2.17	Tresca yield surface	42
2.18	von Mises yield surface	44

2.19	Tresca and von Mises yield surfaces	44
2.20	Three-dimensional yield shape	45
2.21	Mohr-Coulomb failure envelope	46
2.22	Mohr-Coulomb failure criterion in stress space	47
2.23	The Drucker-Prager yield surface	48
2.24	The Drucker-Prager yield criterion	49
2.25	Modified Drucker-Prager/cap model: yield surfaces	50
2.26	Void ratio Vs $\ln \sigma'_v$ relationship	52
2.27	Drained peak and ultimate strength	53
2.28	Critical strength	54
2.29	Triaxial compression and extension tests	57
2.30	State boundary surface for Cam clay	58
2.31	Yield curve for Cam-clay	58
2.32	The Cam clay yield locus and the flow rule	60
3.1	Confined uniaxial test cell with drain holes	69
3.2	Groove geometry	70
3.3	Confined uniaxial compression	71
3.4	Single pass SRI shredder	71
3.5	Fibre determination apparatus	72
3.6	Flat platen response at 1mm/min & 1mm/min	74
3.7	Experimental scheme	74
3.8	Flat platen responses at 2mm/min	76
3.9	Grooved platen responses at 1mm/min	77
3.10	Instron uniaxial testing machine	79
3.11	Quasi-static response for flat platen	82
3.12	Quasi-static response for 35° platen	83

3.13	Uniaxial compression	86
3.14	One-dimensional compression and swelling	87
3.15	Uniaxial results with triaxial tests	90
4.1	Comparison of permeability responses	98
4.2	Permeability cell apparatus	100
4.3	Measured permeability responses	102
4.4	Comparison of permeability test results	104
5.1	Behaviour of ideal linear elastic material	110
5.2	Elastic and plastic compression	112
5.3	Behaviour of ideal perfectly plastic materials	115
5.4	Yielding and plastic straining	117
5.5	Behaviour during a cycle of loading	117
5.6	Hardening and softening of Cam-clay	119
5.7	Capped Drucker-Prager model	121
5.8	Precompression apparatus	127
5.9	Stress path for the initial yield	127
5.10	Quarter cell symmetry	129
5.11	Quasi-static experimental responses	131
5.12	Strain hardening responses	131
5.13	Strain hardening responses for the platens	132
6.1	Some typical displacement pore pressure elements	140
6.2	Porous elastic volumetric behaviour	143
6.3	Boundary conditions for a test cell	146
6.4	Boundary conditions for a roll mill	146
6.5	Contact pressure-clearance relationships	148

6.6	Meshes of varying desity that were studied	150
6.7	Mesh for rezoning	155
6.8	Physical and computational domain	157
7.1	Advanced milling facility	162
7.2	Two-roll (groove) experimental mill scheme	165
7.3	Two-roll geometry	166
7.4	Directly measured and effective permeabilities	168
7.5	Roll load and torque for roller speed $S= 0.15$ m/s	171
7.6	Two-roll symmetry at half groove depth	172
7.7	Modification of yield surface for higher initial void ratios	174
7.8	Recommended modifications for the permeability	176
7.9	Pressure distribution along flank of tooth	177
7.10	Softened pressure-overclosure relationship	179
7.11	Displaced mesh at different compression ratios	180
7.12	Comparative response of roll load to compression ratio	181
7.13	Comparative response of roll load to surface speed	181
7.14	Comparative response of roll torque to compression ratio	182
7.15	Comparative response of roll torque to surface speed	183
7.16	Comparative responses of roll load at $S= 0.15$ m/s	184
7.17	Comparative responses of roll torque at $S= 0.15$ m/s	184
7.18	Predicted Mises stress and volumetric strain	186
7.19	Predicted void ratio and pore pressure	187
7.20	Predicted fibre and juice velocity vectors	188
7.21	Effect of blanket height and feed pressure	190
7.22	Strain hardening responses for different M	190
7.23	Effect of M on speed ratio	191

7.24	Two-roll (flat) mill experimental scheme	193
7.25	Flat platen response and strain hardening response	195
7.26	Comparison of roll load and torque	196
7.27	Measured x -velocities at $C= 2.82$	197
7.28	Predicted feed velocities at $C= 2.82$	198
8.1	Three-dimensional formation	201
8.2	Blanket in 3-dimensions	203
8.3	Stress and void ratio at $C= 3.0$	204
8.4	Inner void ratio and pore pressure at $C= 3.0$	204
8.5	Juice and fibre velocity vectors for a 3-D blanket	204
8.6	Groove penetration and stress variation	205
8.7	Roll loads from 3-D simulation	206
8.8	Roll torques from 3-D simulation	207
9.1	Geometry of a three-roll mill pressure feeder	211
9.2	Geometrical relationship	212
9.3	Roll load and torque traces	214
9.4	Principal stress vectors	215
9.5	Juice and fibre velocity vectors for a 3-roll	216
9.6	Adapted mesh for rezoning	216

List of symbols

α	Contact angle
α_a	Angle of contact between feed chute and rolls
α, β, γ, J	Geometrical coefficients in elliptic equation
β	Material's angle of friction
ϵ	Total strain vector
ϵ^e	Elastic strain
ϵ^p	Plastic strain
ϵ_s^p	Plastic shear strain
$\epsilon_v^p, \epsilon_v^{pl}$	Plastic volumetric strains
ϵ^t	Total strain
ϵ_h	Horizontal strain
ϵ_s	Shear strain
ϵ_s^e	Elastic shear strain
ϵ_{vn}	Volumetric strain at $C=1$
ϵ_v, ϵ_p	Volumetric strain
ϵ_v^e	Elastic volumetric strain
ϵ_v^p	Plastic volumetric strain
$\epsilon_x, \epsilon_y, \epsilon_z$	Strains in x, y, z directions, respectively
η, μ	Dynamic viscosity
Γ	Slope of the specific volume at $p'=0$
γ_f	Unit weight of fluid
$\gamma_{xy}, \gamma_{yz}, \gamma_{zx}$	Shear strains

κ	Slope of Swelling Recompression Line (SRL)
λ	Slope of Normal Compression Line (NCL)
μ	Friction factor
ν	Poisson's ratio
ϕ	Angle at neutral plane
ϕ	Angle of internal friction
ϕ	Slope in the τ/σ plane
ϕ'_{crit}	Soil friction angle
ρ	Density of solid-fluid mixture
ρ_c	Density of cane
ρ_f	Density of fibre
ρ_j	Density of juice
ρ_l	Density of liquid
ρ_{ng}	No gas density
ρ_s	Density of solid
σ'	Normal effective stress
σ	Total normal stress
$\sigma_1, \sigma_2, \sigma_3$	Principle stresses
σ_{av}	Average stress
σ_e	Effective stress
σ_e	von Mises equivalent stress
σ_h	Horizontal stress
σ_n	Normal stress
σ'_v	Normal effective stress
$\sigma_x, \sigma_y, \sigma_z$	Normal stresses
σ_Y	Yield stress
σ_z	Vertical stress

τ, τ_f	Shear stresses
τ_{max}	Maximum shear stress
$\tau_{xy}, \tau_{yz}, \tau_{zx}$	Shear stresses
θ	Angular position in mill measured from axial plane
θ_1, θ_2	Angular positions for roll arc surface
v	Specific volume
v_f	Final specific volume
v_o	Initial specific volume
ξ, η	Computational domain coordinates
1, 2, 3	Spatial coordinate directions
A	Cross sectional area
A_p	Cross sectional area of test cell
A_s	Specific surface area
A_v	Cross sectional area of voids
\hat{a}	Treatment number
b	Length
C	Compression ratio
C_θ	Compression ratio as a function of angular position
C_c	Slope in the $e/\ln \sigma'$ plane, Corrected compression ratio
C_i	Initial compression ratio
C_o	Reference or mill compression ratio
c	Contact clearance
D	Roll diameter
d	Groove depth
d	Material cohesion
E	Extraction fraction

E, E'	Young's modulus
e	Void ratio
e_o	Initial void ratio
F	Force
F_c	Compaction
F_r	Filling ratio
F_r	Radial force
F_t	Tangential force
F_v	Vertical force
f	Fibre ratio
f_o	Reference fibre ratio
G, G'	Shear modulus
G_α	Grooving angle
g	Gravitational constant
h	Height of specimen
h	Pressure head
h_θ	Height as a function of θ
h_θ	Total height between the rolls
h_f	Height of feed chute
h_{ng}	No gas height
h_o	Blanket height
h_o	Initial height of specimen
$h_{s\theta}$	Height of solid material
i	Gradient or head loss
J_1, J_2	First and second stress invariants
K	Permeability
K	Re-absorption factor

K, K'	Bulk modulus
K_e	Effective permeability
K_o	Coefficient of lateral pressure
K_s, K_l	Bulk moduli of solid and liquid phases
k	Coefficient of permeability
k	Darcy coefficient matrix of permeability
L, l	Lengths
l_b	Cane blanket length
M	Slope of the q/p' plane
m_f	Mass of fibre
N	Torque-load number
n	Porosity
\bar{P}	Global liquid pressure
P	Pore pressure
P, Q	Mesh control functions
P_a	Pressure in the axial direction, psi
P_b	Yield locus
P_l	Liquid pore pressure
P_t	Total fluid pressure
p	Mean stress
p	Pressure, Contact pressure
p'	Mean normal effective stress
p_t^e	Elastic tensile stress
p_m	Mean load per unit area
p_o	Initial pressure
p_t	Tensile stress
p'_y	Yield stress

Q	Volume flow rate
q	Deviator stress
q'	Effective shear stress
\dot{q}	Crushing rate
R	Residual error
R	Roll separating force
S	Platen speed, Roll surface speed
S	Speed of piston
S_f	Feed velocity
S_l	Degree of liquid saturation
S_o	Set opening
S_r	Relative rubbing speed
T	Roll torque
T_{tot}	Total torque
T_x, T_y	Traction forces in x and y direction
t	Deviatoric stress measure
t	Thickness
t	time
\ddot{u}	Solid phase acceleration
$\dot{\bar{u}}$	Global velocity vector for the solid
u	Displacement for the solid
u	Pore pressure
u_x, u_y	Displacements in x and y direction
V	Average velocity of liquid
V	Total volume or sample volume
V_b	Volume of bagasse
V_c	Volume of cane

V_f	Volume of fibre
V_j	Volume of juice
V_{ng}	No gas volume
V_{ref}	Reference volume
V_s	Volume of solid
V_v	Volume of voids
V_w	Volume of liquid
\dot{V}_b	Volume rate of bagasse
\dot{V}_e	Escribed volume rate of juice
\dot{V}_f	Volume rate of fibre
\dot{V}_{je}	Volume rate of juice
\dot{V}_j	Total volume rate of juice
\dot{V}_{ng}	No void volume rate of juice
v	Superficial velocity
v	Velocity
v_v	Seepage velocity
v_x, v_y	Velocities in x and y direction
v_y	Vertical compression speed
w	Uncertainty
w	Weighting function
\dot{w}	Liquid velocity vector
w_{dh}	Uncertainty in differential head
w_{av}	Uncertainty in vertical stress
w_A	Uncertainty in area
w_c	Uncertainty in compression ratio
w_d	Work opening at delivery nip
w_f	Work opening at feed nip

w_h	Uncertainty in height of specimen
w_k	Uncertainty in permeability
w_l	Uncertainty in length
w_{ng}	Uncertainty in no gas height
w_o	Work opening
w_Q	Uncertainty in flow rate
w_{F_v}	Uncertainty in vertical force
x, y, z	Spatial coordinate directions